Structures and electronic properties of platinum nitride by density functional theory

Jamal Uddin and Gustavo E. Scuseria
Department of Chemistry, Rice University, Houston, Texas 77005-1892, USA
(Received 20 January 2005; revised manuscript received 8 March 2005; published 1 July 2005)

We present the results of ground state electronic structure calculations of the zinc-blende and rocksalt phases of binary platinum nitride (PtN) using density functional theory. Several exchange-correlation functionals including the local spin density approximations, generalized gradient approximations (GGA), a nonempirical meta-GGA, and a screened Coulomb hybrid functional have been employed. We use Gaussian type orbitals within the framework of periodic boundary conditions. Our results confirm earlier findings, in that the zinc-blende structure of PtN is energetically more stable than the rocksalt structure. The predicted energy difference between the two phases is rather small with the more elaborate functionals. Both phases are predicted to be metallic and extended Pt *d*-N *p* hybridizations are found in both of them. We have also calculated the phase transition pressure between both phases. The bulk modulus of the zinc-blend phase of PtN is significantly higher than that of bulk platinum.

DOI: 10.1103/PhysRevB.72.035101 PACS number(s): 71.20.Ps, 81.05.Zx

I. INTRODUCTION

Transition-metal nitrides are commonly referred to as refractory metals that possess an unusual combination of physical and chemical properties.[1] Due to their outstanding mechanical, optical, and magnetic properties they have received increasing attention in recent years. These materials can be used as corrosion resistants and optical coatings, electrical contacts and diffusion barriers, and in many other technological applications. They are also of much interest in catalysis,[2] electrode materials for batteries and fuel-cells,[3] and superconductors.[4]

Platinum forms simple binary compounds such as halides, oxides, and chalcogenides, but it was not known to form nitrides previously.[5] Among Ni, Pd, and Pt, only nickel[6] forms a nitride with stoichiometry of Ni_3N.[6,7] Therefore there has been considerable interest in the synthesis of platinum nitrides. Recently, Gregoryanz *et al.*[8] reported the discovery of platinum nitride (PtN), the first binary nitride of the noble metals group. It was found that the compound has a remarkably high bulk modulus of 372 GPa, which is about 100 GPa higher than that for pure Pt.[8] Early members of first row transition metal nitrides are known to have rocksalt structures where metal atoms retain a fcc lattice while nitrogen atoms occupy the octahedral interstitial sites. In the case of some late transition metal nitrides, the structures were found to be zinc-blende type, where the fcc metals and nitrogen atoms are tetrahedrally coordinated.[9]

From a theoretical perspective, it is interesting to carry out investigations on structural properties of the PtN. There exists extensive theoretical calculations on the stability and electronic structures of many transition metal nitrides.[10–26] The most notable of them is the calculations on 1:1 binary 3*d*-5*d* transition metal nitrides by Häglund and co-workers[21,22,24] based on the combination of thermodynamic data analysis and the linear muffin-tin orbital (LMTO) method. These calculations were carried out only on rocksalt type structures and alternative structures were not reported.

In this work, we are interested in studying the ground-state properties of PtN and have employed some recently developed state-of-the-art density functional theory (DFT) methodology. We report calculated properties such as lattice constants (a_0), bulk moduli (B_0), and cohesive energies (E_{coh}) for zinc-blende and rocksalt phases of PtN. We predict the phase transition pressure (P_T) between them and discuss their electronic density of states (DOS). We use Gaussian type orbitals (GTOs) and exchange and correlation functionals that include meta-generalized gradient approximation (meta-GGA) and hybrid functionals in addition to the conventional local spin density approximation (LSDA) and GGA. Very recently, Sahu and Kleinman reported relativistic full-potential linear augmented plane wave (FLAPW) calculations with augmented plane wave (APW) basis[10] on PtN using the PBE functional.[27] As discussed below, in agreement with our own PBE results, these authors predict that the zinc-blende phase of PtN is more stable than the rocksalt phase, and that PtN is metallic. However, our calculated energy difference between the zinc-blende and the rocksalt phases with meta-GGA (TPSS) and hybrid (HSE) functionals are significantly lower compared to LSDA and PBE.

II. COMPUTATIONAL DETAILS

We have carried out all calculations using a periodic boundary conditions (PBC) algorithm[28] implemented in the GAUSSIAN suite of programs.[29] This PBC code makes use of GTOs in a linear combination of atomic orbitals-crystal orbital (LCAO-CO) framework.

For nitrogen, we have used a 6-31G(d) basis set (10*s*4*p*1*d*) and for platinum, an energy optimized valence basis set developed by ourselves. Sixty core electrons ([Kr]$4d^{10}4f^{14}$) were replaced with the small-core relativistic effective core potentials (RECP) of the Stuttgart and Dresden group.[30] We optimized the valence basis set for Pt considering 5*s*, 5*p*, 5*d*, 6*s*, and 6*p* orbitals and keeping exponents of the most diffuse *s* and *p* functions at 0.10.[31] The optimized exponents and contraction coefficients of this new basis set are presented in Table I.

TABLE I. Energy optimized exponents (α_i) and contraction coefficients (d_i) of Gaussian functions for platinum used in the present work (Ref. 31). The basis set has a 3111/2211/41 contraction scheme.[a]

Shell type	Exponents (α)	Coefficients (d)
s	15.67780876	−1.11548332
	14.66986238	1.36519580
	5.85050683	−0.64106567
	1.22836002	1.00000000
	0.52214442	1.00000000
	0.10000000	1.00000000
p	7.94953519	4.91357550
	7.31409602	−5.94276414
	1.68103481	0.19733727
	0.87295990	0.23702023
	0.37093650	1.00000000
	0.10000000	1.00000000
d	3.64261965	−0.58260049
	3.49285803	0.59819400
	1.14285490	0.18582882
	0.44988116	0.18589774
	0.15343324	1.00000000

[a]Atomic HF energy for this basis set =−118.382641 (a.u.), original (311111/22111411) basis set −118.388721 (a.u.).

A set of four exchange-correlation functionals representing different families chosen for comparison are the LSDA realization includes Slater exchange (S)[32] with correlation from Vosko, Wilk, and Nusair (VWN5);[33] the PBE-GGA;[27] the nonempirical meta-GGA recently developed by Tao, Perdew, Staroverov, and Scuseria (TPSS),[34] and the screened Coulomb hybrid functional developed by Heyd, Scuseria, and Ernzerhof (HSE).[35,36]

We have used 784 k-points in the Brillouin zone integration for all the calculations. Partial charges were determined using Mulliken population analysis. We performed all calculations with unit cells that are double the size of primitive cells. This arrangement let us test different magnetic configurations. However, for all calculations reported in this paper we have used a closed-shell configuration within the unit cell and to describe a nonmagnetic phase of PtN.[37] The zinc-blende and rocksalt unit cells used in our PBC calculations are shown in Fig. 1. Equilibrium bulk properties a_0, B_0, and its pressure derivatives B', as well as the total energy at equilibrium were determined using all nonhybrid (LSDA, PBE, and TPSS) and hybrid (HSE) functionals by fitting total energy vs volume data into the third order Birch-Murnaghan equation of state (EOS).[38] These data were obtained from a set of volumes over a range of values around equilibrium. The DOS were calculated using all four functionals. The bulk properties of the most stable fcc phase of platinum have been calculated for this work in the same way as in the case of PtN.

The PtN cohesive energy (E_{coh}) is calculated as the difference between the total energy of PtN and its isolated constituent atoms as

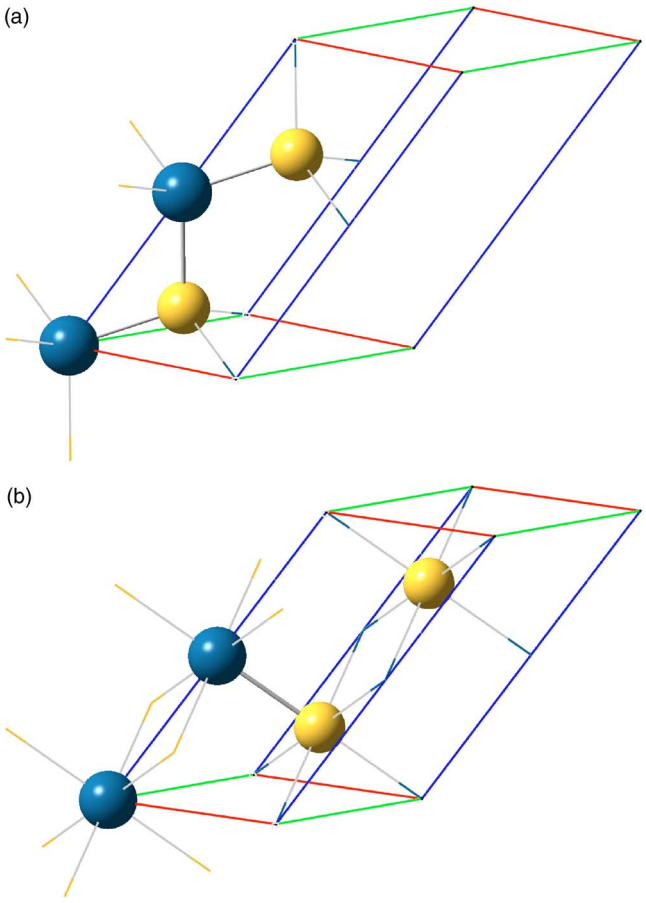

FIG. 1. (Color online) Unit-cell for the zinc-blende and rocksalt structures. Darker spheres denote platinum atoms. Tetrahedral and octahedral environments are apparent from the atomic orientations.

$$E_{coh}(\mathrm{PtN}) = (E_{\mathrm{Pt}}^{\mathrm{atom}} + E_{\mathrm{N}}^{\mathrm{atom}}) - E_{\mathrm{PtN}}^{\mathrm{solid}}.$$

We report average cohesive energy per atom for PtN, which is the same quantity above divided by 2. For platinum, E_{coh} is calculated in a similar way. A positive value for E_{coh} indicates an exothermic reaction for forming the solid.

III. RESULTS AND DISCUSSION

The calculated equilibrium values for a_0, Pt—N and Pt—Pt distances, as well as B_0 and B' for the PtN phases are given in Table II together with the experimental values for the zinc-blende type structure. The a_0 values calculated with PBE and TPSS agree very well with the experimental result while LSDA and HSE predict shorter values. The predicted nearest-neighbor Pt—N distance is shorter in the zinc-blende phase compared to the rocksalt phase. An opposite trend is seen for the Pt—Pt distances at each level of theory. Our PBE calculated values for lattice constants for the zinc-blende and the rocksalt structures are very close (within 0.004 Å) to the values reported by Sahu and Kleinman using the FLAPW method and APW basis.[10] The slight difference can be attributed to differences in the implementation (basis set, treatment of core electrons, etc.).

In Table II the calculated a_0, Pt—Pt distance, B_0, and B' values are also shown for bulk platinum. There is an excel-

TABLE II. Calculated lattice constants a_0, Pt—N and Pt—Pt bond lengths (all in Å), bulk moduli B_0 (in GPa), and its dimensionless pressure derivative B' of phases of bulk PtN and bulk fcc platinum.

	a_0	Pt—N	Pt—Pt	B_0	B'	V_0B_0
			zinc-blende (PtN)			
LSDA	4.711	2.040	3.331	462	4.95	12076
PBE	4.801	2.079	3.395	373	5.06	10319
TPSS	4.794	2.076	3.390	389	4.95	10715
HSE	4.761	2.062	3.367	417	5.02	11262
Experimental	4.804	2.080	3.397	372	5.26	10311
			rocksalt (PtN)			
LSDA	4.429	2.215	3.132	548	4.95	11902
PBE	4.521	2.261	3.197	438	5.02	10118
TPSS	4.504	2.252	3.185	473	4.92	10804
HSE	4.468	2.234	3.159	511	4.92	11398
			bulk platinum			
LSDA	3.928		2.778	292	5.308	
PBE	4.002		2.830	235	5.272	
TPSS	3.975		2.811	259	5.212	
Experimental	3.924		2.775	266	5.8	

lent agreement between the experimental and LSDA a_0 values. If we compare a_0 and the Pt—Pt distance for bulk Pt with those for PtN, we find that intercalation of N atoms in the interstitial spaces increases the lattice vector as well as the Pt—Pt distance of fcc platinum which is located within the PtN structure. The increase of Pt—Pt distances, however, is larger in the zinc-blende than in the rocksalt type structure.

It is interesting to note that for bulk PtO, LSDA predicts lattice constants that are closer to the experimental values than those obtained with PBE.[39] As mentioned above, the opposite is predicted for the zinc-blende phase of PtN.

The PBE and TPSS calculated values for B_0 of the zinc-blende phase are 373 and 389 GPa, respectively. The experimentally observed bulk modulus of PtN is 372 GPa.[8] LSDA seems to largely overestimate the bulk modulus of PtN. Significant overestimation is found for HSE as well. The overall B_0 of the rocksalt phase is much higher than that of the zinc-blende phase. The LSDA calculated B_0 is 110, 75, and 37 GPa higher than the PBE, TPSS, and HSE calculated values, respectively. Our PBE results for B_0 are in good agreement with those reported by Sahu and Kleinman using the FLAPW method and APW basis.[10]

In the case of bulk platinum, LSDA overestimates, PBE underestimates, and TPSS agrees well with the experimental B_0 value of 266 GPa. Bulk modulus (volume stiffness) is sometimes correlated to hardness,[40] especially for cubic materials.[41] It is seen that B_0 for PtN in the zinc-blende type structure increases by 170, 138, and 130 GPa compared to the corresponding values for bulk platinum using LSDA, PBE, and TPSS, respectively. Therefore our predictions indicate that PtN is likely to be much harder than Pt. It can be seen in Table II that approximately the same V_0B_0 values are found for both phases at any given level of theory. This is consistent with the empirical $B \propto 1/V$ law.[42,43]

The E_{coh} values for PtN and Pt solids along with the experimental value for bulk Pt are shown in Table III. Large cohesive energies of PtN phases indicate stability of the solids compared to the constituent atoms. However, the E_{coh} for the zinc-blende phase is only 0.17, 0.23, 0.07, and 0.06 eV/PtN higher than that of the rocksalt phase according to LSDA, PBE, TPSS, and HSE, respectively. This indicates higher stability of the zinc-blende type structure by a small margin with the meta-GGA and hybrid functionals.

Sahu and Kleinman predicted values for E_{coh} in each phase that are 0.3 eV/atom smaller compared to our calculated values with PBE.[10] However, the difference in E_{coh} between the two phases is the same (~0.2 eV). LSDA systematically overestimates E_{coh} compared to GGA by about 1.3 eV compared to PBE in both PtN phases. The E_{coh} values for the other two functionals are comparable. In the case of bulk Pt, LSDA overbinds by 1.4 eV compared to experiment.

TABLE III. Calculated cohesive energy (E_{coh}),[a] of phases of bulk PtN and bulk fcc Pt (in eV/atom).

	LSDA	PBE	TPSS	HSE	Experimental
zinc-blende (PtN)	5.53	4.26	4.03	3.35	
rocksalt (PtN)	5.36	4.03	3.96	3.29	
Pt	7.21	5.59	5.75		5.852

[a]Positive values indicate exothermic reactions.

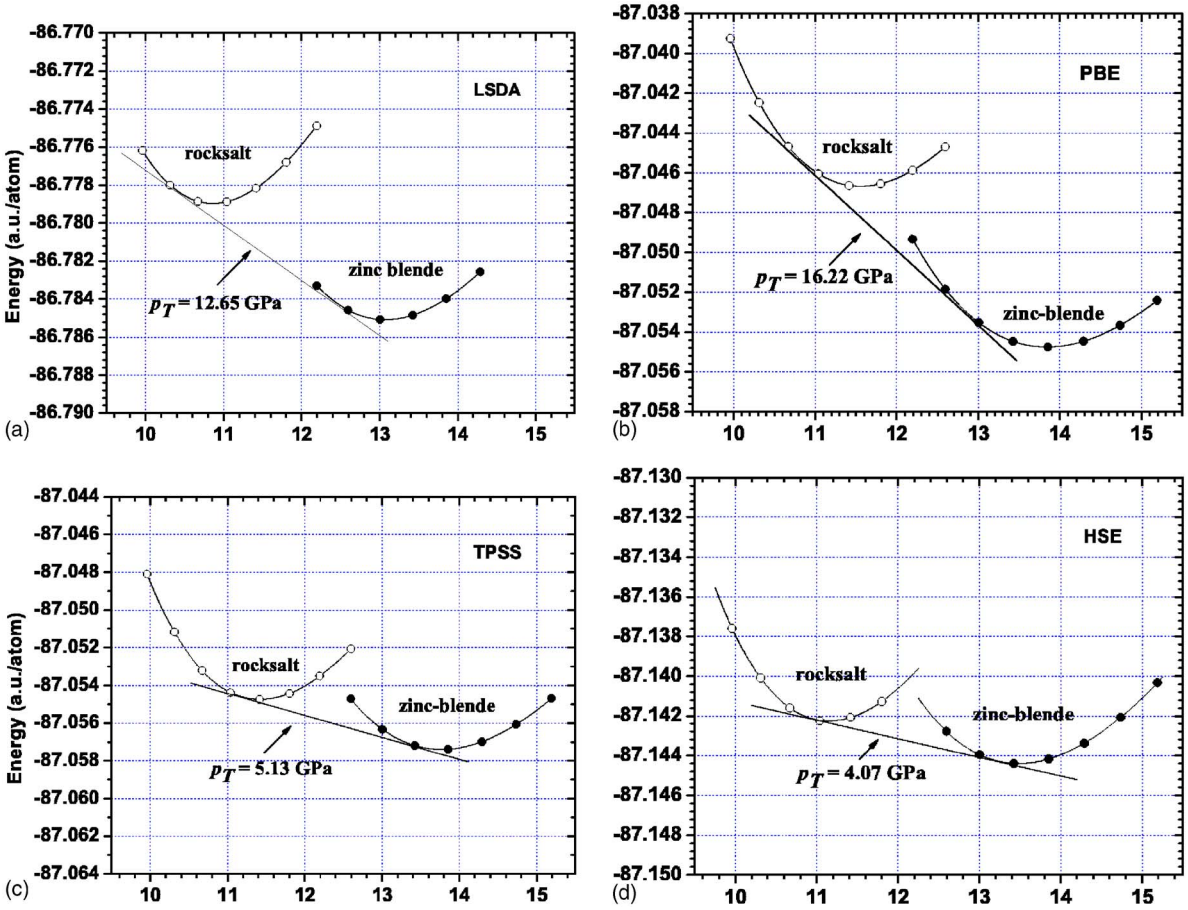

FIG. 2. Total energy (a.u. per unit cell) vs volume (Å^3) for the zinc-blende and the rocksalt phases of PtN with the LSDA, PBE, TPSS, and HSE functionals. The fitted curves are obtained using Birch-Murnaghan equation of states. Transition pressures are calculated from the common tangents connecting two curves at each level of theory.

The PBE and TPSS functionals produce approximately similar cohesive energies that are in good agreement with the experimental value.[44]

The transition pressures (P_T) calculated from the common tangent connecting the energy versus volume curves of the rocksalt and the zinc-blende type structures are illustrated in Fig. 2 for all functionals. The total energy versus volume curves are obtained from Birch-Murnaghan EOS fittings. The fact that PtN is energetically more stable in the zinc-blende than in the rocksalt structure is evident in Fig. 2. The common tangent shown for PBE has a slope of -3.72×10^{-3} a.u./Å^{-3}, which is equivalent to a transition pressure of 16.2 GPa. For the transition to take place, a pressure equal to or greater than 12.7, 16.2, 5.2, and 4.1 GPa is needed at the LSDA, PBE, TPSS, and HSE levels, respectively. The phase transition pressure predicted by Sahu and Kleinman with PBE[10] is in excellent agreement with our corresponding result. Note that the correct phase transition pressure in Ref. 10 is 17.5 GPa instead of 24 GPa.[45] TPSS and HSE predict smaller transition pressures of the order of 4 to 5 GPa. No experimental phase transition pressure is available for comparison.

The DOS obtained with the nonhybrid functionals are almost identical. We therefore present only the DOS for PBE and HSE in Fig. 3. The Fermi energies are shown by dashed vertical lines at 0 eV. PtN is predicted to be metallic at all levels of theory. In both phases, the use of HSE reduces the DOS slightly at the Fermi energy compared to the PBE calculated ones. In a recent study of PtO,[39] we found that a band

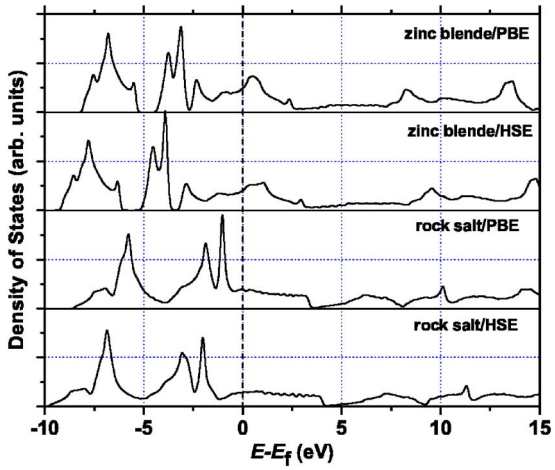

FIG. 3. The total density of states (DOS) of the zinc-blende and the rocksalt phases of PtN calculated using PBE and HSE functionals. The Fermi level is placed at 0 eV and marked by a dashed vertical line.

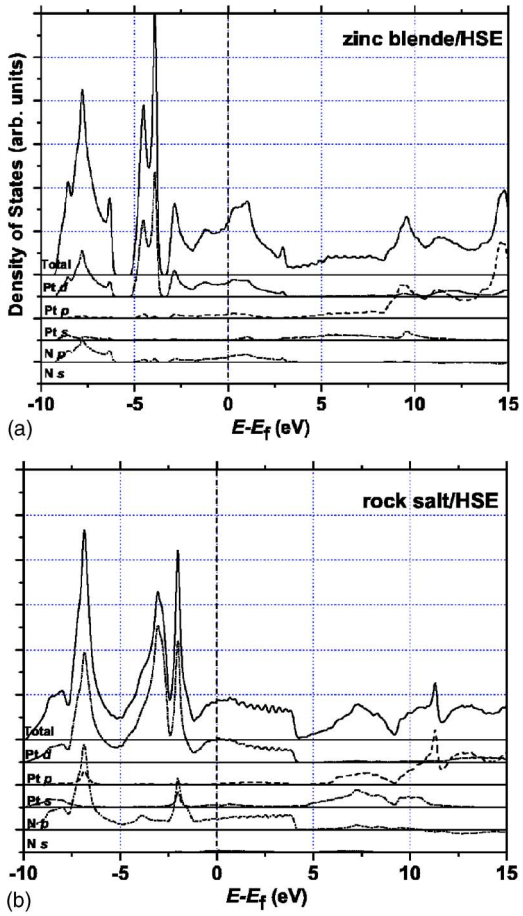

FIG. 4. The total and partial density of states (DOS) for PtN calculated using the HSE functional for the zinc-blende phase (left figure) and the rocksalt phase (right figure). The Fermi level is placed at 0 eV and marked by a dashed vertical line in each case.

gap at the Fermi level appears when hybrid HSE is used instead of nonhybrid functionals. The latter predicts PtO to be a metal. Our calculated DOS share similar characteristics to that of other transition metal nitrides.[11,12,18,19,22]

To gain more insight into the bonding nature of PtN phases, *s*-, *p*-, and *d*- state resolved partial density of states obtained with the HSE functional are presented in Fig. 4. In both types of structures, the DOS between approximately −10 and 5 eV are primarily composed of N *p* orbitals and Pt *d* orbitals. This results in extended hybridizations between Pt *d* and N *p* orbitals. In the 0 eV to −5 eV region, the contribution from N *p* is not prominent. In the rocksalt phase, however, there exists a smaller peak between −2.5 and −1.0 eV made of N *p* orbitals. The other peak in this region is mostly from pure Pt *d*-orbitals. In the conduction level just above the Fermi energy, Pt *d* and N *p*-orbitals are the biggest contributors.

Partial charges are obtained from Mulliken population analysis. All functionals predict a Pt partial charge of 0.8 to 0.9 for the zinc-blende structure and a much smaller charge (0.5 to 0.7) for the rocksalt structure. This indicates a stronger charge transfer in the zinc-blende type structure.

IV. CONCLUDING REMARKS

We have performed a systematic study of the ground state electronic structures of the zinc-blende and the rocksalt phases of PtN using density functional theory and Gaussian type functions with periodic boundary conditions. Exchange correlation functionals, representing four different families, have been used. All functionals predict the zinc-blende type structure to be energetically more stable than the rocksalt type structure. We confirm both phases of PtN to be a metallic conductor. The zinc-blende phase has a very large bulk modulus, which is approximately 100 GPa higher than pure platinum. The phase transition pressure is predicted to be low, but varies largely with different functionals.

We find reasonably good agreement between all functionals for lattice parameters and electronic density of states. The PBE predicted lattice constant is the closest to the experiment value. However, for a benchmark set of solids, TPSS and HSE perform better than PBE.[46,47] Interestingly, PBE in the case of PtN, and LSDA in the case of bulk Pt, show better agreement with experiment. LSDA usually overestimates and GGA underestimates the bulk moduli,[48–50] and this seems valid for bulk Pt but not for PtN. PBE reproduces the experimental value for PtN which is overestimated by LSDA.

Relative to GGA, LSDA generally underestimates phase transition pressures.[51–53] This is observed in the case of PtN as well where the PBE predicted value for the phase transition is 3.5 GPa higher than LSDA. Although TPSS and HSE agree well with each other, their predicted transition pressures (which are in the order of 5 GPa) are three times smaller than the PBE value. These lower transition pressures originate primarily from the significantly smaller energy difference between two phases predicted by TPSS and HSE.

ACKNOWLEDGMENTS

This work was supported by the Department of Defense (DoD) through a Multidisciplinary University Research Initiative (MURI) grant managed by the Army Research Office (ARO). We are grateful to Professor Leonard Kleinman for his help regarding the calculation of phase transition pressures.

[1] L. E. Toth, *Transition Metal Carbides and Nitrides* (Academic Press, New York, 1971).

[2] S. Tsubota, M. Haruta, T. Kobayashi, A. Ueda, and Y. Nakahara, in *Preparation of Catalysts V*, edited by G. Poncelet, P. A. Jacobs, P. Grange, and B. Delmon (Elsevier, Amsterdam, 1991).

[3] M. Keijzer, K. Hemmes, J. H. W. De Wit, and J. Schoonman, J. Appl. Electrochem. **30**, 1421 (2000).

[4] L. Francavilla, S. A. Wolf, and E. F. Skelton, IEEE Trans. Magn.

17, 569 (1981).
[5] N. Greenwood and A. Earnshaw, in *Chemistry of the Elements* (Butterworth-Heinemann, London, 1997).
[6] A. Leineweber, H. Jacobs, and S. Hull, Inorg. Chem. **40**, 5818 (2001).
[7] S. Krishnamurthy, M. Montalti, M. G. Wardle, M. J. Shaw, P. R. Briddon, K. Svensson, M. R. C. Hunt, and L. Ŝiller, Phys. Rev. B **70**, 045414 (2004).
[8] E. Gregoryanz, C. Sanloup, M. Somayazulu, J. Badro, G. Fiquet, H.-K. Mao, and R. J. Hemley, Nat. Mater. **3**, 294 (2004).
[9] K. Suzuki, T. Kaneko, H. Yoshida, H. Morita, and H. Fujimori, J. Alloys Compd. **224**, 232 (1995).
[10] B. R. Sahu and L. Kleinman, Phys. Rev. B **71**, 041101(R) (2005).
[11] P. Lukashev and W. R. L. Lambrecht, Phys. Rev. B **70**, 245205 (2004).
[12] B. R. Sahu and L. Kleinman, Phys. Rev. B **68**, 113101 (2003).
[13] C. Stampfl, W. Mannstadt, R. Asahi, and A. J. Freeman, Phys. Rev. B **63**, 155106 (2001).
[14] M. Marlo and V. Milman, Phys. Rev. B **62**, 2899 (2000).
[15] J.-Q. Li, Y.-F. Zhang, S.-C. Xiang, and Y.-N. Chiu, J. Mol. Struct.: THEOCHEM **530**, 209 (2000).
[16] J. C. Grossman, A. Mizel, M. Côté, M. L. Cohen, and S. G. Louie, Phys. Rev. B **60**, 6343 (1999).
[17] A. Filippetti, W. E. Pickett, and B. M. Klein, Phys. Rev. B **59**, 7043 (1999).
[18] B. Eck, R. Dronskowski, M. Takahashi, and S. Kikkawa, J. Mater. Chem. **9**, 1527 (1999).
[19] H. Shimizu, M. Shirai, and N. Suzuki, J. Phys. Soc. Jpn. **66**, 3147 (1997).
[20] L. I. Johansson, Surf. Sci. Rep. **21**, 177 (1995).
[21] A. F. Guillermet, J. Häglund, and G. Grimvall, Phys. Rev. B **48**, 11673 (1993).
[22] J. Häglund, A. Fernandez Guillermet, G. Grimvall, and M. Körling, Phys. Rev. B **48**, 11685 (1993).
[23] A. Fernandez Guillermet, J. Häglund, and G. Grimvall, Phys. Rev. B **45**, 11557 (1992).
[24] J. Häglund, G. Grimvall, T. Jarlborg, and A. F. Guillermet, Phys. Rev. B **43**, 14400 (1991).
[25] A. F. Guillermet and G. Grimvall, Phys. Rev. B **40**, 10582 (1989).
[26] D. A. Papaconstantopoulos, W. E. Pickett, B. M. Klein, and L. L. Boyer, Phys. Rev. B **31**, 752 (1985).
[27] J. P. Perdew, K. Burke, and M. Ernzerhof, Phys. Rev. Lett. **77**, 3865 (1996).
[28] K. N. Kudin and G. E. Scuseria, Phys. Rev. B **61**, 16440 (2000).
[29] Gaussian Development Version, Revision B.07, and C.01, M. J. Frisch, G. W. Trucks, H. B. Schlegel, G. E. Scuseria, M. A. Robb, J. R. Cheeseman, J. A. Montgomery Jr., T. Vreven, K. N. Kudin, J. C. Burant, J. M. Millam, S. S. Iyengar, J. Tomasi, V. Barone, B. Mennucci, M. Cossi, G. Scalmani, N. Rega, G. A. Petersson, H. Nakatsuji, M. Hada, M. Ehara, K. Toyota, R. Fukuda, J. Hasegawa, M. Ishida, T. Nakajima, Y. Honda, O. Kitao, H. Nakai, M. Klene, X. Li, J. E. Knox, H. P. Hratchian, J. B. Cross, C. Adamo, J. Jaramillo, R. Gomperts, R. E. Stratmann, O. Yazyev, A. J. Austin, R. Cammi, C. Pomelli, J. W. Ochterski, P. Y. Ayala, K. Morokuma, G. A. Voth, P. Salvador, J. J. Dannenberg, V. G. Zakrzewski, S. Dapprich, A. D. Daniels, M. C. Strain, O. Farkas, D. K. Malick, A. D. Rabuck, K. Raghavachari, J. B. Foresman, J. V. Ortiz, Q. Cui, A. G. Baboul, S. Clifford, J. Cioslowski, B. B. Stefanov, G. Liu, A. Liashenko, P. Piskorz, I. Komaromi, R. L. Martin, D. J. Fox, T. Keith, M. A. Al-Laham, C. Y. Peng, A. Nanayakkara, M. Challacombe, P. M. W. Gill, B. Johnson, W. Chen, M. W. Wong, C. Gonzalez, and J. A. Pople, Gaussian, Inc., Wallingford CT, 2004.
[30] D. Andrae, U. Haeussermann, M. Dolg, H. Stoll, and H. Preuss, Theor. Chim. Acta **77**, 123 (1990).
[31] The basis set used was energy optimized in conjunction with the small-core 1997 relativistic ECP in the same way as the original Stuttgart basis set but fixing the exponent of the most diffuse *s* and *p* functions at 0.10. In this way, we avoid numerical linear dependencies originated by the presence of diffuse (small exponent) functions.
[32] J. C. Slater, *Quantum Theory of Molecules and Solids*; Vol. 4 (McGraw-Hill, New York, 1974).
[33] S. H. Vosko, L. Wilk, and M. Nusair, Can. J. Phys. **58**, 1200 (1980).
[34] V. N. Staroverov, G. E. Scuseria, J. Tao, and J. P. Perdew, J. Chem. Phys. **119**, 12129 (2003).
[35] J. Heyd, G. E. Scuseria, and M. Ernzerhof, J. Chem. Phys. **118**, 8207 (2003).
[36] J. Heyd and G. E. Scuseria, J. Chem. Phys. **120**, 7274 (2004).
[37] PtN is electronically more delocalized than nonmagnetic PtO and/or bulk Pt. Therefore PtN is expected to be nonmagnetic as well.
[38] F. Birch, Phys. Rev. **71**, 809 (1947).
[39] J. Uddin, J. E. Peralta, and G. E. Scuseria, Phys. Rev. B **71**, 155112 (2005).
[40] J. M. Legér and B. Blanzat, J. Mater. Sci. Lett. **13**, 1688 (1994).
[41] A. Y. Liu, R. M. Wentzcovitch, and M. L. Cohen, Phys. Rev. B **38**, 9483 (1988).
[42] R. M. Hazen and L. W. Finger, J. Geophys. Res. **84**, 6723 (1979).
[43] J. A. Majewski and P. Vogl, Phys. Rev. B **35**, 9666 (1987).
[44] C. Kittel, *Introduction to Solid State Physics* (Wiley, New York, 1986).
[45] L. Kleinman (private communication).
[46] J. Heyd and G. E. Scuseria J. Chem. Phys. **121**, 1187 (2004).
[47] V. N. Staroverov, G. E. Scuseria, J. Tao, and J. P. Perdew, Phys. Rev. B **69**, 075102 (2004).
[48] P. H. T. Philipsen and E. J. Baerends, Phys. Rev. B **61**, 1773 (2000).
[49] A. D. Corso, A. Pasquarello, A. Baldereschi, and R. Car, Phys. Rev. B **53**, 1180 (1996).
[50] M. Fuchs, M. Bockstedte, E. Pehlke, and M. Scheffler, Phys. Rev. B **57**, 2134 (1998).
[51] N. Moll, M. Bockstedte, M. Fuchs, E. Pehlke, and M. Scheffler, Phys. Rev. B **52**, 2550 (1995).
[52] D. R. Hamann, Phys. Rev. Lett. **76**, 660 (1996).
[53] J. Kang, E.-C. Lee, and K. J. Chang, Phys. Rev. B **68**, 054106 (2003).